Supporting Information

Tobler et al. 10.1073/pnas.0809599106

SI Methods

Participants. Fifteen right-handed healthy participants (mean age, 27 years; range, 20–41 years; 8 females) were investigated in experiment 1, 14 (mean, 25 years; range: 20–30 years, 6 females) in experiment 2. For experiment 1, the individual participants, the basic design of the experiments, and the imaging techniques for recording the hemodynamic response of reward regions were identical to those previously reported (1). All participants were preassessed to exclude prior histories of neurological or psychiatric illness. Participants gave informed consent, and the study was approved by the Joint Ethics Committee of the National Hospital for Neurology and Neurosurgery (U.K.).

Behavioral Procedure. In both experiments, participants were placed on a moveable bed in the scanner with light head restraint to limit head movement during image acquisition. Participants viewed a computer monitor through a mirror fitted on top of the head coil.

Experiment 1 consisted of an imperative paradigm, which allowed us to study the processing of expected value and risk independent of choice. Participants pressed one of 4 buttons corresponding to the spatial quadrant of stimulus presentation. We determined individual risk attitudes in a separate rating task outside the scanner (see following text). At the beginning of a trial in the main paradigm, single visual stimuli appeared for 1.5 s in one of the 4 quadrants of the monitor. Outcomes appeared 1 s after the stimulus for 0.5 s below the stimulus on the monitor such that outcome and stimulus presentation coterminated. Intertrial intervals varied between 1 and 8 s according to a Poisson distribution with a mean of 3 s. In each trial, we randomly presented one of 12 visual stimuli, each predicting reward (points) with a specific magnitude and probability. Ten of these 12 stimuli were of special interest for the present study. We used four levels of expected value, which varied between 50 and 200 points in steps of 50. For each of these levels, we used a high- and a low-risk variant with the same expected value, resulting in 8 different stimuli. The remaining 2 stimuli of special interest were those predicting reward at $p = 0.0$, which were used to analyze risk-independent value coding together with the 2 stimuli predicting reward at $p = 1.0$. The 2 stimuli of less interest were 100 at $p = 0.25$ and $p = 0.75$, which served only for comparison of different risk terms. The stimuli and the rewarded versus unrewarded outcomes alternated randomly within the boundaries defined by the probabilities (48 trials for $p = 1.0$; e.g., 36 rewarded and 12 unrewarded trials for $p = 0.75$); thus, producing a measured mean of reward identical to the expected value. Throughout the experiment, the total points accumulated were displayed and updated in rewarded trials at the time of reward delivery; 4% of the total points were predictably paid out as British pence at the end of the experiment.

The visual stimuli were specific combinations of attributes drawn from 2 visual dimensions, shape and color, indicating reward magnitude and probability, with 1 dimension indicating reward magnitude and the other probability. For example, 4 orange circles could predict 400 points with $p = 0.5$, whereas 2 dark red circles could predict 200 points with $p = 1.0$. Both stimuli were associated with different combinations of magnitude and probability but the same expected value (200 points). We counterbalanced the meaning of dimensions (shape or color of stimuli) and the direction in which they changed (for shape, number of circles per stimulus; for color, relative level of yellow or red) across participants. Stimulus delivery was controlled using Cogent 2000 software (Wellcome Department of Imaging Neuroscience, London, U.K.) as implemented in Matlab 6.5 (Mathworks).

The expected value and risk associated with the 10 stimuli of interest were calculated according to the following formulae: expected value (EV) $= \Sigma_i\ (m_i \times p_i)$; risk $= [\Sigma_i\ (m_i - \mathrm{EV})^2]/n$, which is equivalent to $p \times (m_i - \mathrm{EV})^2 + (1 - p) \times (0 - \mathrm{EV})^2$. In the formulae, m is magnitude of reward, p is probability of reward, and n is number of elements (outcomes associated with each stimulus). The number of elements is $n = 1$, 2, or 4 for $p = 0.0$ or 1.0, $p = 0.5$, and $p = 0.25$ or 0.75, respectively.

The procedure comprised a training and a testing phase. In the training phase, participants learned the meaning of the stimuli and how to perform the task while each stimulus was presented in 8 consecutive trials. Earnings in the training phase did not contribute to the monetary earnings of participants, but accumulated points were nevertheless displayed. Participants were in the scanner during the training phase while structural scans were taken. Functional data were acquired in the test phase, comprising 2 sessions, each with 24 randomly alternating presentations of each stimulus. The task remained the same as during the training phase, but outcomes contributed to total earnings. In both training and testing phase, stimuli appeared in one of the 4 quadrants of the screen. The quadrant of stimulus appearance varied randomly between trials. Participants were instructed to press one of 4 buttons corresponding to the spatial quadrant of stimulus presentation. If they failed to press the correct button within 900 ms, the trial was aborted, a red "X" appeared, and 100 points were subtracted from the accumulated earnings. Error trials were repeated, and reported results correspond to correct trials in the testing phase.

Participants rated the pleasantness of visual stimuli before and after the experiment on a scale ranging from 5 = very pleasant to −5 = very unpleasant. We evaluated ratings statistically by repeated-measures ANOVA. An interaction analysis between trial type and time (before and after the experiment) tested for changes in pleasantness ratings induced by the procedure. Also, we quantified probabilistic risk aversion by comparing the post-experimental ratings for ($p = 0.25 + p = 0.75$) and $p = 1.0$ (2, 3). If the rating for ($p = 0.25 + p = 0.75$) is smaller than, the same as, or larger than the one for ($p = 1.0$), then the particular individual is risk averse, risk neutral, or risk-seeking, respectively. Thus, in experiment 1, the principal measure of risk attitude was imperative and did not rely on choice because experiment 1 was imperative and did not involve choice.

We used a secondary, choice-based, measure of risk attitude to determine whether there was a relation with the imperative measure. For the secondary measure, we tested preference of participants between 2 concurrently presented stimuli, both before and after the experiment. Participants chose between stimuli associated with low- and high-risk, but the same expected value. Each time the participant chose the less risky stimulus after the experiment, the factor of risk aversion increased by 1, whereas choosing the riskier stimulus decreased it by 1 ($n = 4$ choices). The factor could range from +4 (strong risk aversion) to −4 (strong risk proneness) with a zero factor corresponding to risk neutrality.

Experiment 2 varied expected value and risk in a choice situation. In each trial, a risky and a safe option appeared for 5.5 s on the right and left side of a fixation cross present in the middle of the screen. Participants had to indicate their choice during the

1-s presentation of a circle around the fixation cross. After the circle disappeared, the chosen option was framed for 1 s. No outcome was shown. Intertrial intervals consisted of a fixed part of 2 s and a variable part, which varied according to an exponential function with a high tail and a mean of 2 s (4). In each trial we randomly presented one of 4 risky options, and a safe option that varied within the range of the risky option it was presented with. We used 2 levels of expected value, 30 and 60£. Each of these was presented in a low- and a high-risk version, with risk varying between 225 and 900£[2]. All choices were recorded. At the end of the experiment, one trial was randomly drawn and participants received the outcome of the drawn trial. If the draw obtained a trial in which participants had chosen a risky option, the option was played out with the toss of a coin. The payout procedure was explained to participants in detail before the experiment.

We used a formal choice-based measure of risk attitudes (5). Specifically, we identified for each risky option the safe amount for which participants were indifferent between the risky and the safe option (certainty equivalent). The certainty equivalent corresponds to the frequency-weighted average of the safe values for which participants at some point during the experiment chose both the risky and safe option. The difference in the certainty equivalents for the high- and low-risk options with the same mean served as index for risk aversion. With this index, only 2 participants were risk-seeking in experiment 2.

Data Acquisition and Analysis. In both experiments, we acquired gradient echo T2*-weighted echo-planar images (EPIs) with blood-oxygen-level-dependent (BOLD) contrast on a Siemens Sonata 1.5 Tesla scanner (slices per volume, 33; repetition time, 2.97 s). Depending on performance of participants, 405–500 volumes (experiment 1) or 327–365 volumes (experiment 2) were collected twice, together with five ''dummy'' volumes at the beginning of each scanning run. In both experiments, scan onset times varied randomly relative to stimulus onset times. A T1-weighted structural image was also acquired for each participant. Signal dropout in basal frontal and medial temporal structures due to susceptibility artifact was reduced by using a tilted plane of acquisition (30 ° to the anterior commissure-posterior commissure line, rostral $>$ caudal) and a z-shim gradient prepulse with a moment of -0.2 mT/m (6). Imaging parameters were: echo time, 50 ms; field-of-view, 192 mm. The in-plane resolution was 3×3 mm; with a slice thickness of 2 mm and an interslice gap of 1 mm. High-resolution T1-weighted structural scans were coregistered to their mean EPIs and averaged together to permit anatomical localization of the functional activations at the group level.

Statistical Parametric Mapping (SPM2 and SPM5; Functional Imaging Laboratory, London, U.K.) served to spatially realign functional data, normalize them to a standard EPI template and smooth them using an isometric Gaussian kernel with a full width at half-maximum of 10 mm. We used a standard rapid event-related fMRI approach in which evoked hemodynamic responses to each trial type are estimated separately by convolving a canonical hemodynamic response function with the onsets for each trial type and regressing these trial regressors against the measured fMRI signal (7, 8). This approach makes use of the fact that the hemodynamic response function summates in an approximately linear fashion over time (9). By presenting trials in strictly random order and using randomly varying intertrial intervals, it is possible to separate out fMRI responses to rapidly presented events without waiting for the hemodynamic response to reach baseline after each single trial (7; 8).

In experiment 1, functional data were analyzed by constructing a set of stick functions at the event-onset times for each of the 12 trial types. Rewarded and unrewarded trial types were modeled separately. The stick function regressors were convolved with a canonical hemodynamic response function (HRF). In separate time course analyses, we made no assumptions about the shape of activations and used 8 finite impulse responses per trial, each response separated from the next by 1 scan (2.97 s). In experiment 2, the onset of the choice options was the event of interest. Trial types were defined by the gamble presented and the choice (risky or safe) made. In both experiments, participant-specific movement parameters were modeled as covariates of no interest.

The general linear model served to compute trial type-specific betas, reflecting the strength of covariance between the brain activation and the canonical response function for a given condition at each voxel for each participant (for detailed descriptions, see ref. 10). The effects of interest (betas, percentage of signal change) were calculated relative to an implicit baseline. Using random-effects analysis, the relevant contrasts of parameter estimates were entered into a series of 1-way *t* tests or simple regressions with nonsphericity correction where appropriate. To control for false positives due to multiple comparisons, we used small volume correction within frontal lobe using the Pickatlas toolbox (FDR at $P < 0.05$) (11). The dependent measure in time course plots is percentage signal change measured at peak voxels, but results were similar in 10-mm volumes around the peak. Reported voxels conform to Montreal Neurological Institute (MNI) coordinate space, with the right side of the image corresponding to the right side of the brain.

1. Tobler PN, O'Doherty JP, Dolan RJ, Schultz W (2007) Reward value coding distinct from risk attitude-related uncertainty coding in human reward systems. *J Neurophysiol* 97:1621–1632.
2. Wakker P (1994) Separating marginal utility and probabilistic risk aversion. *Theory and Decision* 36:1–44.
3. Gonzalez R, Wu G (1999) On the shape of the probability weighting function. *Cog Psychol* 38:129–166.
4. Hagberg GE, Zito G, Patria F, Sanes JN (2001) Improved detection of event-related functional MRI signals using probability functions. *Neuroimage* 14:1193–1205.
5. Luce RD (2000). *Utility of Gains and Losses* (Lawrence Erlbaum, Mahway, NJ).
6. Weiskopf N, Hutton C, Josephs O, Deichmann R (2006) Optimal EPI parameters for reduction of susceptibility-induced BOLD sensitivity losses: A whole-brain analysis at 3 T and 1.5 T. *Neuroimage* 33:493–504.
7. Dale AM, Buckner RL (1997) Selective averaging of rapidly presented individual trials using fMRI. *Hum Brain Mapp* 5:329–340.
8. Josephs O, Henson RN (1999) Event-related functional magnetic resonance imaging: Modelling, inference and optimization. *Philos Trans R Soc Lond B* 354:1215–1228.
9. Boynton GM, Engel SA, Glover GH, Heeger DJ (1996) Linear systems analysis of functional magnetic resonance imaging in human V1. *J Neurosci* 16:4207–4221.
10. Friston KJ, et al. (1995) Statistical parametric maps in functional imaging: A general linear approach. *Hum Brain Mapp* 2:189–210.
11. Maldjian JA, Laurienti PJ, Burdette JH, Kraft RA (2003) An automated method for neuroanatomic and cytoarchitectonic atlasbased interrogation of fMRI data sets. *Neuroimage* 19:1233–1239.

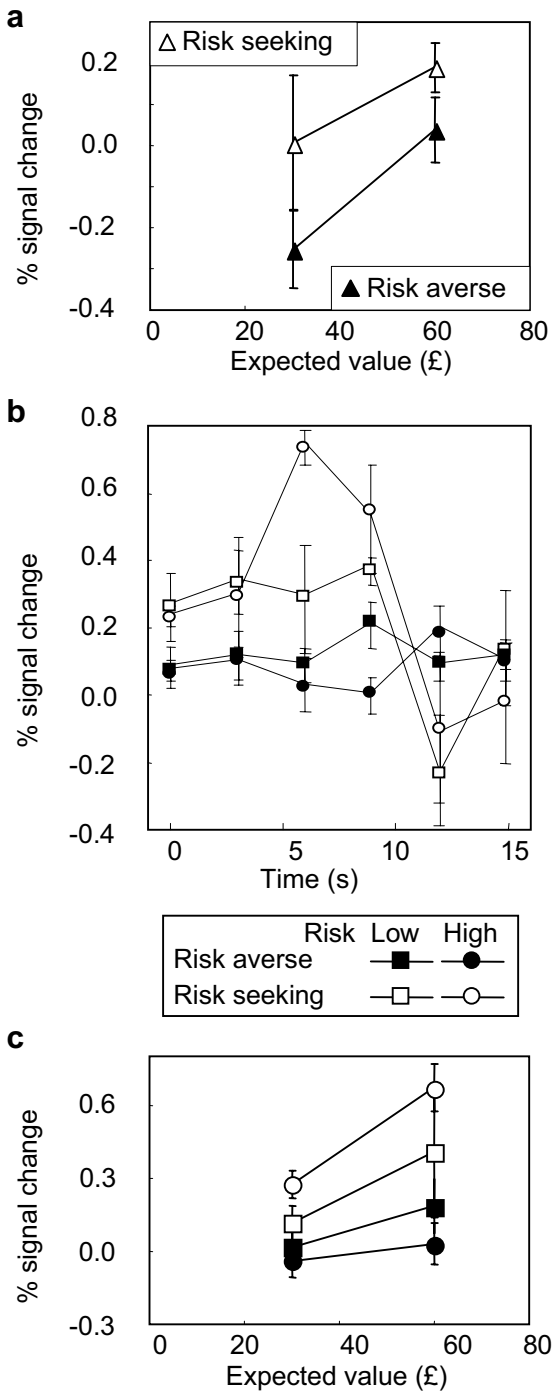

Fig. S1. Integration of value and risk during choice (experiment 2). (*a*) Increase with expected value in safe options irrespective of risk attitude. Peak activations from cluster shown in Fig. 3*A* covarying with expected value for risk-averse and risk-seeking individuals. Activations increased with expected value ($P < 0.05$, paired *t* test across groups). The differences between the groups were not significant ($P \geq 0.33$, unpaired *t* tests). (*b*) Risk attitude-dependent modulation of responses to risky options in lateral prefrontal cortex in choice experiment 2. Time courses of responses were extracted from circled cluster shown in Fig. 3*A*. Options were associated with different levels of risk (average variance of low- and high-risk options, 312.5 and 650£^{2}). Responses were averaged separately for risk-averse and risk-seeking participants and across the 2 levels of expected value used (30 and 60 £; average, 45 £). (*c*) Peak activations from time course analysis shown in *b*, averaged separately for risk-averse and risk-seeking participants. Activations were moderately higher with higher risk in risk-seeking participants and moderately lower in risk averse participants. This resulted in significant activation differences between the 2 groups for the high risk, but not for the low-risk options (high risk, $t = -3.9$, $P < 0.01$; low risk, $t = -1.14$, $P = 0.27$, unpaired *t* tests). Across groups, activations increased with expected value ($t = 2.2$, $P < 0.05$, paired *t* tests).

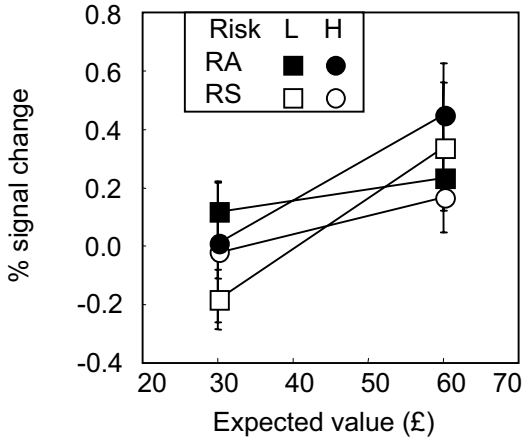

Fig. S2. Risk-independent striatal value coding in second, choice, experiment. Activation increased significantly with expected value in close proximity to peak voxel detected in imperative experiment ($P < 0.05$, small volume correction with false discovery rate in 10-mm sphere around peak voxel shown in Fig. 4*A*). There were no significant differences between groups for low- and high-risk options ($t \leq 0.6$, $P \geq 0.54$). RA, risk averse; RS, risk seeking; L, low; H, high.